European Drag Reduction and Flow Control Meeting – EDRFCM 2015
March 23–26, 2015, Cambridge, UK

RIBLET DRAG REDUCTION AND THE EFFECT OF BULK FLUID ROTATION IN A FULLY TURBULENT TAYLOR-COUETTE FLOW

A.J. Greidanus, R. Delfos, S. Tokgöz, J. Westerweel
Laboratory for Aero and Hydrodynamics, Faculty of Mechanical, Maritime and Materials Engineering,
Delft University of Technology, The Netherlands

INTRODUCTION

Low drag surfaces are often desired in many industries with applications in open and closed channel flows, such as ship hulls and pipe flows. Drag reduction is a phenomenon that can have substantial energy savings, resulting in ecological and economical benefits.

We use a Taylor-Couette facility as experimental instrument to measure the drag change of turbulent wall-bounded flows above modified surfaces [2, 4]. In this manuscript, we apply a riblet surface to observe the drag change compared to a smooth reference surface. Riblets are small surface protrusions which are aligned in the flow direction. They reduce drag by disturbing the spanwise motion of the flow at the surface and thereby moving turbulent vortices further away from the wall [1]. The turbulent flow is investigated via tomo-PIV measurements, which identify the change in flow structures and velocity profile of the flow between two counter-rotating cylinders.

EXPERIMENTAL SETUP

The experimental setup consists of two coaxial closed cylinders that both can rotate independently and was used in previous investigations [3, 5]. The radius of the inner cylinder is $r_i = 110$ mm and total length $L_i = 216$ mm. The outer cylinder has a radius $r_o = 120$ mm and length $L_o = 220$ mm. The inner cylinder is assembled within the outer cylinder with high precision; the gap between the two cylinders in radial direction (TC-gap) and in axial direction (vK-gap) is $d = r_o - r_i = 10.0$ mm and $h = (L_o - L_i)/2 = 2.0$ mm, respectively. Hence, the radial gap ratio is $\eta = r_i/r_o = 0.917$ and axial aspect ratio is $\Gamma = L_i/d = 21.6$.

The desired angular velocities of the inner and outer cylinders were regulated by two independent motors that were controlled by a software program. The torque M on the inner cylinder was recorded with a co-rotating torque meter (abs. precision ± 0.01 Nm) that is assembled in the shaft between the driving motor and inner cylinder. The torque and rotation rate signal of the inner cylinder were recorded at a sampling rate of 2 kHz for 120 seconds. The outside wall temperature T_{out} of the outer cylinder was recorded by an infrared-thermometer and the fluid temperature T_f was indirectly determined via heat transfer calculations to indicate the fluid viscosity during operation.

Tomographic particle image velocimetry was used to measure the three velocity components in the instantaneous flow field. The application of tomo-PIV to a Taylor-Couette setup is described in more detail by Tokgöz *et al.* [5]. PIV measurements were conducted of a volume between the two cylinders over a FOV of roughly 40 × 20 × 10 mm^3 in axial, azimuthal and radial directions. The measurement volume was located at mid-height of the rotational axis to minimize the possible end effects of the Taylor-Couette facility on the measurements.

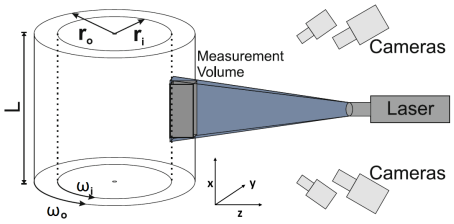

Figure 1: Experimental setup [5]; Taylor-Couette facility and PIV system. The coordinate system in the measurement volume is given by x for axial, y for azimuthal and z for radial direction.

PIV AND TORQUE MEASUREMENTS WITH RIBLET SURFACE

Global rotation can enhance or suppress turbulence for only inner or outer cylinder rotation respectively [6]. Therefore, the measurements were performed under exact counter-rotation $\omega_o r_o = -\omega_i r_i$ with increasing angular velocities and results in similar flow conditions as for boundary layer or fluid channel experiments. The shear stress on the surface was determined by $\tau_w = M/(2\pi r_i^2 L_i)$. The applied riblets have a triangular cross-section geometry, with a spacing $s = 120$ μm and height $h = \pm 110$ μm, and were applied in azimuthal direction on the inner cylinder surface only, as it is much easier, faster and more accurate.

Figure 2 presents the drag change $\Delta\tau/\tau_0$ as a function of the shear Reynolds number Re_s, which is given by $Re_s = U_{sh} d/\nu$ with $U_{sh} = \omega_o r_o - \omega_i r_i$ and ν is the fluid viscosity. The friction was reduced for a Reynolds number $4.0 \times 10^3 < Re_s < 8.5 \times 10^4$. The drag increase in the Taylor vortices regime ($Re_s < 4.0 \times 10^3$) is supposed to be the results of the presence of large-scale structures with relative large axial flow motions, indicated by PIV measurements (Fig.3). For $Re_s > 8.5 \times 10^4$ the riblets are considered as surface roughness and loose their drag reducing benefits.

The core of the flow shows very low azimuthal velocities and indicates an averaged bulk velocity $\bar{U}_b = 0$ for the reference case (Fig.4, $*$), where the surface of the inner and outer cylinder are identical and makes the rotation number $R_\Omega = 0$ [3].

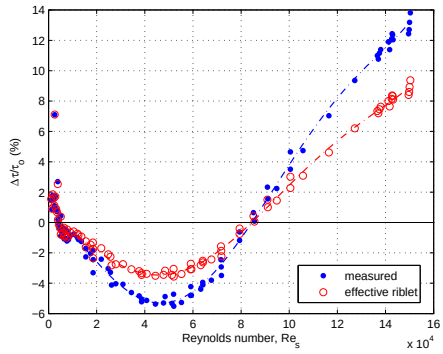

Figure 2: Drag change by riblet inner cylinder under exact counter-rotation ($R_\Omega = 0$) *vs.* shear Reynolds number Re_s.

A rotation effect occurs when the inner and outer cylinder surfaces have different wall-bounded flow conditions and modifies the rotation number R_Ω. Riblets on the inner cylinder wall reduced the drag with 5.3% at $Re_s = 4.7 \times 10^4$ and the averaged *bulk* fluid started to co-rotate slightly with the direction of the outer cylinder (Fig.4, ∘).
The shift in averaged bulk velocity of $\delta = \bar{U}_b/U_{out}$ was determined by $\delta = (1 - \sqrt{(1 + \Delta\tau/\tau_0)})/(1 + \sqrt{1 + \Delta\tau/\tau_0})$ and a maximum drag reduction of 5.3% corresponds to an averaged bulk velocity $\delta = 0.014$, which was confirmed by PIV measurements (inset Fig.4). The shift $\delta = 0.014$ agrees to an apparent rotation number $\hat{R}_\Omega = 0.0012$, which is very small but sufficient enough to play a substantial role in the total measured drag change [2, 3]. This rotation effect influence the drag already with -1.9%, resulting to an effective riblet drag reduction of 3.4% (Fig.2).

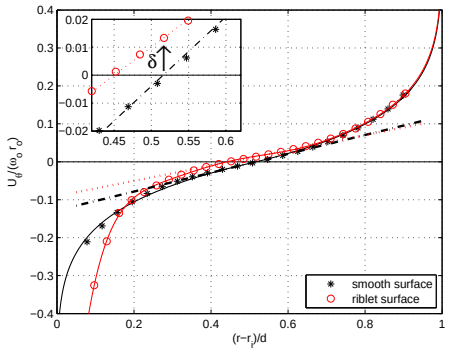

Figure 4: Mean normalized velocity profile of smooth and riblet surfaces at $Re_s = 4.7 \times 10^4$, under exact counter-rotation conditions. Inset: Zero-crossing of the azimuthal velocity.

REFERENCES

[1] DW Bechert, M Bruse, W Hage, JG Th Van der Hoeven, and G Hoppe. Experiments on drag-reducing surfaces and their optimization with an adjustable geometry. *Journal of Fluid Mechanics*, 338:59–87, 1997.

[2] AJ Greidanus, R Delfos, S Tokgöz, and J Westerweel. Turbulent Taylor-Couette flow over riblets: Drag reduction and the effects of bulk fluid rotation. Submitted to Experiments in Fluids.

[3] Florent Ravelet, Rene Delfos, and Jerry Westerweel. Influence of global rotation and Reynolds number on the large-scale features of a turbulent Taylor-Couette flow. *Physics of Fluids (1994-present)*, 22(5):055103, 2010.

[4] Siddarth Srinivasan, Justin A Kleingartner, Jonathan B Gilbert, Robert E Cohen, Andrew JB Milne, and Gareth H McKinley. Sustainable Drag Reduction in Turbulent Taylor-Couette Flows by Depositing Sprayable Superhydrophobic Surfaces. *Physical Review Letters*, 114(1):014501, 2015.

[5] S Tokgöz. *Coherent Structures in Taylor-Couette Flow: Experimental Investigation*. PhD thesis, TU Delft, Delft University of Technology, 2014.

[6] LJA Van Bokhoven, HJH Clercx, GJF Van Heijst, and RR Trieling. Experiments on rapidly rotating turbulent flows. *Physics of Fluids (1994-present)*, 21(9):096601, 2009.

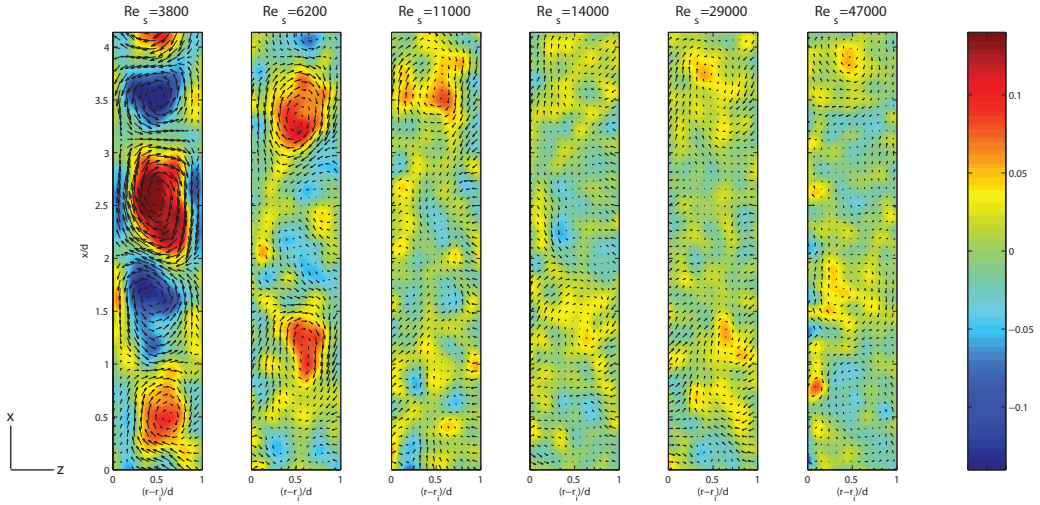

Figure 3: Vorticity plot: Color indicates the normalized strength of the out-of-plane vorticity $\bar{\omega}_z/(\omega_o r_o/d)$, arrows indicate the radial and axial velocities. The velocity in each plot is normalized to outer cylinder wall velocity $\omega_o r_o$.